Internal structures of scaffold-free 3D cell cultures visualized by synchrotron radiation-based micro computed tomography

Belma Saldamli*[a,b], Julia Herzen[c], Felix Beckmann[c], Jutta Tübel[d], Johannes Schauwecker[d], Rainer Burgkart[d], Philipp Jürgens[b], Hans-Florian Zeilhofer[b], Robert Sader[a], and Bert Müller[e]
[a]Oral, Cranio-Maxillofacial and Facial Plastic Surgery, J.W. Goethe University, 60590 Frankfurt am Main, GERMANY;
[b]Hightech Research Center of Cranio-Maxillofacial Surgery, University Hospital Basel, 4031 Basel, SWITZERLAND;
[c]GKSS-Research Center, 21502 Geesthacht, GERMANY;
[d]Department of Orthopedic Surgery, Klinikum r. d. Isar, TU München, 81675 Munich, GERMANY;
[e]Biomaterials Science Center, University of Basel, 4031 Basel, SWITZERLAND

ABSTRACT

Recently the importance of the third dimension in cell biology has been better understood, resulting in a re-orientation towards three-dimensional (3D) cultivation. Yet adequate tools for their morphological characterization have to be established. Synchrotron radiation-based micro computed tomography (SRμCT) allows visualizing such biological systems with almost isotropic micrometer resolution, non-destructively. We have applied SRμCT for studying the internal morphology of human osteoblast-derived, scaffold-free 3D cultures, termed histoids. Primary human osteoblasts, isolated from femoral neck spongy bone, were grown as 2D culture in non-mineralizing osteogenic medium until a rather thick, multi-cellular membrane was formed. This delicate system was intentionally released to randomly fold itself. The folded cell cultures were grown to histoids of cubic milli- or centimeter size in various combinations of mineralizing and non-mineralizing osteogenic medium for a total period of minimum 56 weeks. The SRμCT-measurements were performed in the absorption contrast mode at the beamlines BW 2 and W 2 (HASYLAB at DESY, Hamburg, Germany), operated by the GKSS-Research Center. To investigate the entire volume of interest several scans were performed under identical conditions and registered to obtain one single dataset of each sample. The histoids grown under different conditions exhibit similar external morphology of globular or ovoid shape. The SRμCT-examination revealed the distinctly different morphological structures inside the histoids. One obtains details of the histoids that permit to identify and select the most promising slices for subsequent histological characterization.

Keywords: three-dimensional cell culture, histoid, synchrotron radiation, micro computed tomography

1. INTRODUCTION

Cell culturing is the basic tool for studying and reproducing biological processes *in vitro*. Application fields vary from fundamental research including cell biology, genetics, and drug discovery to clinical such as tissue engineering and industrial utilization i.e. pharmacology and cosmetics. Tissue culture emerged in the beginning of the 20th century as a method for studying the behavior of animal cells free of systematic variations that might arise *in vivo*.[1] The technique was elaborated first to aggregated fragments of tissue under growth conditions restricted to cell migration from the periphery including occasional mutations. This type of culturing dominated about 50 years until its rapid replacement by the spread culture, established from disaggregated tissue, a.k.a. two-dimensional (2D) cell culture. Recently, the importance of the extra-cellular matrix (ECM) and the third dimension in cell biology has been better understood, resulting in an increasing interest and re-orientation towards histotypic and organotypic culturing, commonly known as three-dimensional (3D) cell cultures.[2] Histotypic/organotypic or 3D cultures provide conditions that maintain important typical *in vivo* properties, such as concomitant growth of multiple cell types, morphological differentiation, formation of histotypical structures, complex spatial organization and homeostatic regulation, which are very difficult and sometimes impossible to achieve by 2D cultures.

*dtbelma@yahoo.com; phone +49 69 6301 5643; fax +49 69 6301 5644

Developments in X-Ray Tomography VI, edited by Stuart R. Stock,
Proc. of SPIE Vol. 7078, 70781X, (2008) · 0277-786X/08/$18 · doi: 10.1117/12.795162

Currently, 3D cultures are being characterized by histological sectioning utilizing staining methods adapted from conventional histology. Unfortunately, the information obtained this way is planar and limited to the rather arbitrarily selected slices, making the evaluation and interpretation of the histoarchitecture of the entire system questionable. Further, the destructive nature of the method restricts the variety of subsequent studies. Therefore, non-destructive methods for the 3D characterization are highly desirable, since viewing on histoarchitectural features of biological systems in 3D provides insights in their complete spatial organization and functionality, which cannot be lonely obtained by conventional histological methods.

Micro computed tomography (μCT) is a valuable non-destructive tool that provides information not only about the outer shape of objects, but also their internal structure. Compared to the conventional μCT, the synchrotron radiation-based micro computed tomography (SRμCT) is set apart by superb contrast as the result of monochromatic x-rays and micrometer resolution that corresponds to the sub-cellular level. For this reason, the latter has attracted interest in the field of cell biology and tissue engineering.[3-7]

The present communication elucidates the power of SRμCT to reveal the micro-architecture of scaffold-free 3D histotypic cultures, derived from human osteoblasts, termed histoids. The present study includes different staining and embedding protocols of the histoids in order to figure out the value of established histological tools for SRμCT. Nevertheless, SRμCT is regarded as complementary to the (immuno-)histochemical methods as demonstrated below.

2. MATERIALS AND METHODS

2.1. Preparation of the histoids

Histotypic cultures of millimeter size derived from human osteoblasts, which could be regarded as pre-state of bony tissue, were grown under static culturing conditions. Briefly, human osteoblasts were isolated from femur neck cancellous bone according to the protocol previously described.[8] The osteoblast cultures were expanded for two passages in Dulbecco's Modified Eagle medium (Biochrom, Berlin, Germany) supplemented with 15% fetal calf serum (Biochrom, Berlin, Germany), 100 mg/l Primocin™ (InvivoGen, San Diego, CA, USA), 10 nM dexamethasone (Sigma, Steinheim, Germany), and 50 μg/ml ascorbic acid (Sigma, Steinheim, Germany). Cells from the second passage were inoculated in T-175 flasks (BD Falcon/Becton Dickinson, New Jersey, USA) and kept at the temperature of 37 °C in a humidified atmosphere containing 5% CO_2. After reaching confluence, the cells were let to proliferate further until multilayered membrane-like structures with obvious loose surface-contact at the flask edges formed. At that time-point, the membranes were carefully detached from the flask bottom with the help of a plastic cell-scraper (BD Falcon/Becton Dickinson, New Jersey, USA) and let to collapse in a randomly folded cluster. After seven days, the clusters were transferred into cell culture dishes (d = 10 cm; BD Falcon/Becton Dickinson, New Jersey, USA) and let to grow under different regiments (Table 1) for at least 56 weeks, in total. During the whole experiment medium was changed weekly.

Table 1. Culturing conditions for the different histoids

	non-mineralizing medium[a]	*mineralizing medium*[b]
Histoid A	80 weeks	-
Histoid B	56 weeks	-
Histoid C	28 weeks	108 weeks
Histoid D	136 weeks	-

[a] *DMEM + 15% FCS + 10 nM dexamethasone + 50 μg/ml ascorbic acid*

[b] *DMEM + 15% FCS + 10 nM dexamethasone + 50 μg/ml ascorbic acid + 10 mM ß-glycerophosphate*

Table 2. Staining and embedding of the different histoids prior to SRμCT

	staining	*embedding*
Histoid A	none	in liquid (Eppendorf container)
Histoid B	osmium tetroxide	paraffin
Histoid C	osmium ammine-B	MMA
Histoid D	osmium ammine-B	paraffin

The histoids were taken from the culture dishes and prepared for the SRμCT-measurements in the following ways. Histoid A was rinsed with phosphate buffered saline (PBS; Sigma Steinheim, Germany) and transferred to a vial with 4% aqueous formaldehyde (Fisher Scientific, Schwerte, Germany) solution. Histoid B was rinsed with cacodylate buffer (0.1 M cacodylic acid solution in PBS, pH 7.4; Sigma, Steinheim, Germany) and then fixated with 0.5% aqueous gluteraldehyde (Polysciences, Inc., Warrington, PA, USA) solution for 3 h at room temperature (RT). Subsequently, the histoid was rinsed again with cacodylate buffer and subjected to labeling and embedding procedures (Table 2). Histoids C and D were rinsed with PBS and then transferred to vials with 4% paraformaldehyde (Merck, Darmstadt, Germany) solution in PBS, pH 7.4, and stored at the temperature of 4 °C until embedding (Table 2).

2.2. Staining methods

2.2.1. Osmium tetroxide (OsO_4)

The staining solution was prepared by diluting 2% OsO_4 (Polysciences, Inc., Warrington, PA, USA) with equal volume of cacodylate buffer, as previously described.[4] The histoid was incubated with the labeling solution for 1 h at RT and finally rinsed in cacodylate buffer.

2.2.2. Osmium ammine-B

The histoids were rinsed with cacodylate buffer (0.1 M cacodylic acid solution in PBS (Sigma, Steinheim, Germany)), at pH 7.4 and then incubated for 1 h at RT in the labeling solution[9] composed of 0.4% osmium ammine-B (Polysciences, Inc., Warrington, PA, USA) dissolved in 40 mM sodium metabisulfite (Aldrich, Deisenhofen, Germany) with 8 M acetic acid (Merck, Darmstadt, Germany). Following this, the histoids were rinsed and incubated with cacodylate buffer at RT for 2 h.

2.3. Embedding of samples

2.3.1. Paraffin embedding

First the histoids were dehydrated incubating in a series of ethanol solutions with increasing concentration (70%, 96% and 100%) (Apotheke, Klinikum r. d. Isar, Munich, Germany) and finally put in xylene (Merck, Darmstadt, Germany), 60 min at RT each step. The histoids were immersed in melted paraffin (Shandon Paraplast, Thermo-Fischer Scientific, Waltham, MA) in pre-heated metallic moulds. The moulds were transferred onto the cold plate to harden. The obtained paraffin blocks were stored at RT until further processing.

2.3.2. Methyl methacrylate (MMA) embedding

For the MMA embedding the Technovit®9100 Kit (Heraeus Kulzer, Wehrheim, Germany) was used. Prior to embedding the histoid was dehydrated as described above. The pre-infiltration and infiltration steps were performed according to the manufacturer's instructions. The sample was let to polymerize at the temperature of 4 °C for 48 h and stored at RT until further processing.

2.4. SRμCT-measurements

The tomograms were acquired at the beamlines BW 2 (Histoids A and D) and W 2 (Histoids B and C) in absorption contrast mode. The tomography experiment at HASYLAB at DESY has been operated by the GKSS-Research Center.[10] The photon energies were adapted to the total absorption of the specimens, namely 10 keV for Histoid A, 26 keV for Histoid B and Histoid C, and 16 keV for Histoid D. The spatial resolution was determined by means of the modulated transfer function of a metal edge.[11] For the Histoids A, B, C, and D these values corresponded to 6.75 μm at the pixel

size of 5.22 µm, 4.19 µm at the pixel size of 2.62 µm, 4.98 µm at the pixel size of 3.30 µm, and 4.04 µm at the pixel size of 2.26 µm, respectively. The tomograms were reconstructed by means of the standard filtered back-projection algorithm[12] usually out of 721 projections acquired from 0 to 180°. For Histoid B the sample rotation axis was asymmetric and the 1441 projections acquired from 0 to 360° were appropriately combined before reconstruction. This approach[13] is helpful to obtain high-resolution data from rather bulky specimens.

2.5. Data processing and visualization

As the histoids were often larger than the field of views, tomograms at different height levels were recorded, namely for Histoids A, B, C, and D seven, four, two and one. Hence, it was necessary to register the individual tomograms and to combine them to finally have one tomogram for each histoid. To keep this procedure as simple as possible, the registration was performed after the reconstruction with voxel size resolution.

The obtained tomograms of the specific histoids were huge. Consequently, for the easier handling and to increase the density resolution (contrast)[5], the data were reduced by the application of binning factors before and after reconstruction. The tomograms of the Histoids A, B, C, and D were binned by the factors of one, two, two, and one before reconstruction and two, two, one, and one after the reconstruction, respectively.

The software VGStudio MAX 1.2.1 (Volume Graphics, Heidelberg, Germany) allowed for the 3D visualization of the tomography data.

2.6. Histological techniques

2.6.1. Histological sectioning

The sections 4 µm thin were cut with a rotary microtome (Leica Microsystems, Wetzlar, Germany) and mounted on glass slides. Prior to histochemical and immunohistochemical examination the sections were deparaffinated by incubation first in xylene and then in a series of ethanol solutions with decreasing concentration (100%, 96%, 70% and 50%), each step 60 min at RT, and finally rehydrated in PBS.

2.6.2. Hematoxylin Eosin (HE) Staining

The deparaffinated and rehydrated sections were incubated in Mayer's Hemalaun[14] for 8 min and then rinsed in running tap water to develop the blue color. The sections were counterstained with 0.1% aqueous eosin for 2 min, rinsed with running tap water and differentiated in 70% ethanol. Then dehydration was performed by incubation in a series of ethanol solutions with increasing concentration (70%, 96% and 100%) and xylene. The slides were coverslipped using Eukitt (VWR, Strasbourg, France).

2.6.3. Masson Goldner Trichrome (MGT) Staining

A standard Masson Goldner Trichrome staining was performed as described by Romeis.[14] Briefly, the deparaffinated and rehydrated sections were incubated in Weigert's solution (Apotheke, Klinikum r. d. Isar, Munich, Germany) for 5 min. After washing with running tap water for 10 min these were stained in a solution of 0.33 g Xylidine Ponceau (Chroma 1B207) with 0.175 g acid fuchsine (Merck 7629) and 1 ml glacial acetic acid (Merck, Darmstadt, Germany) in 500 ml distilled water for 7 min. Then the sections were briefly rinsed in 0.3% acetic acid (Merck, Darmstadt, Germany) and stained in a solution of 15 g phosphomolybdic acid (Merck Nr. 583) and 10 g Orange G (Merck Nr. 6878) in 500 ml distilled water for 5 min, again briefly rinsed in 0.3% acetic acid, and counterstained with a solution of 0.5 g Light Green (Merck 1315) and 1 ml glacial acetic acid in 500 ml distilled water for 2 min. Finally, these were soaked in 0.3% acetic acid for 5 min. The sections were dehydrated in ethanol solutions with increasing concentration and xylene. The slides were coverslipped using Eukitt.

2.6.4. Immunohistochemical staining of collagen type I (col I) and collagen type IV (col IV)

Briefly, the deparaffinated and rehydrated sections were treated with a 1% H_2O_2 aqueous solution for 10 min at RT to block the endogenous peroxidase activity. Col I antigen retrieval was done by incubation in 0.04% pepsin (Sigma, Deisenhofen, Germany) in 0.01 N HCl for 90 min at RT. Col IV was unmasked by heat-induced epitope retrieval (HIER). Precisely, the sections were incubated in Target Retrieval Solution, pH 6.1 (Dako, Hamburg, Germany) and heated in a microwave oven with the electrical powers of 500, 400, and 250 W for the periods of 5 min each. The primary antibodies (Abs), mouse polyclonal anti-collagen I (Quartett, Berlin, Germany) and rabbit polyclonal anti-collagen IV (Dako, Hamburg, Germany) were used at a dilution of 1:25 and 1:75, respectively. The samples were

incubated in the primary Abs at RT, either overnight (col I) or for 1 h (col IV). After washing, the sections were incubated in the biotinylated secondary anti-mouse Ab or anti-rabbit Ab (both Dianova, Hamburg, Germany; dilution 1:200) for 30 min at RT. Detection was done by incubation in avidin/biotin peroxidase complex using the Vectastain ABC Elite Kit (Vector Laboratories, Birlingane, CA) for 30 min at RT. The sections were developed using the AEC+ substrate-chromogen (Dako, Hamburg, Germany). Counterstaining was done by immersing in Mayer's Hemalaun for 90 s. The slides were coverslipped using Kaisers glycerol jelly (Merck, Darmstadt, Germany).

3. RESULTS AND DISCUSSION

Histoid A was natively scanned, i.e. without the application of any contrast agent, immersed in 4% formaldehyde solution. It was transported and measured within an Eppendorf container. After SRμCT-measurement, it was embedded into paraffin. The micrometer-thin sections were histochemically and immunohistochemically stained. SRμCT in absorption contrast mode does not provide sufficient contrast for the detailed evaluation of the cellular structures. One can only identify well-defined spherical features of cell size that exhibit lower of X-ray absorption than the surrounding tissue and liquid (see Fig. 1). These features correlate well with the size, number and localization/distribution pattern of the adipocytes in the histological sections.

It should be mentioned that the transition regions between the individually acquired tomograms are visible because of the reduced photon density at the periphery.

About the rather large, higher x-ray absorbing features we can only speculate, since the unique registration between the histological slices and virtual cuts of the tomography data has been impossible.

Therefore, Histoid B was stained with OsO_4 and embedded into paraffin prior to the SRμCT-measurements. OsO_4 is a lipid stain commonly used in optical, secondary electron, and transmission electron microscopy. The substance readily reacts with and binds to intracellular and membrane lipids. The strongly x-ray absorbing osmium significantly change the total absorption of the histoid and requires much higher photon energies for SRμCT visualization. Histoid B appears as a spheroid-nodular core wrapped in a membrane-like structure. This part of the histoid is connected to tail-like membranous components that seem to originate from the feeder layer of the 3D culture as shown in the images of Fig. 2.

As for Histoid A, one finds spherically shaped features that are associated with the osmium stained intracellular lipids of adipocytes (bright because of high x-ray absorption). These are predominantly located on the surface of the nodular part and in the loosely accompanying tail-like structures.

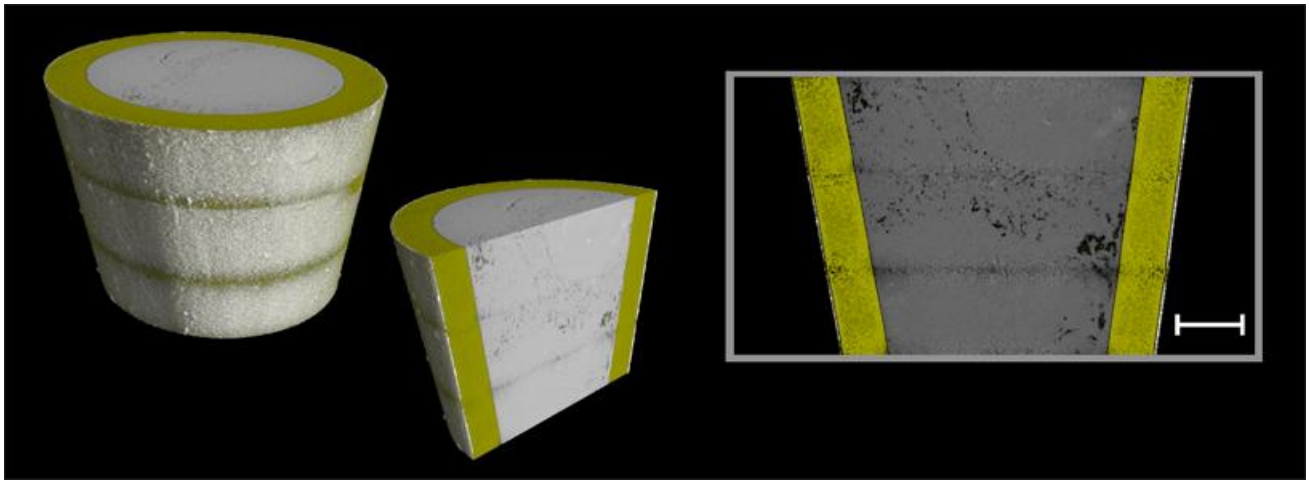

Fig. 1. The 3D visualization of the SRμCT data of Histoid A shows spherically shaped features that are even better visualized in the virtual cut (inset). The yellow coloring for the Eppendorf container is added to enhance the available information. The bar corresponds to 1 mm.

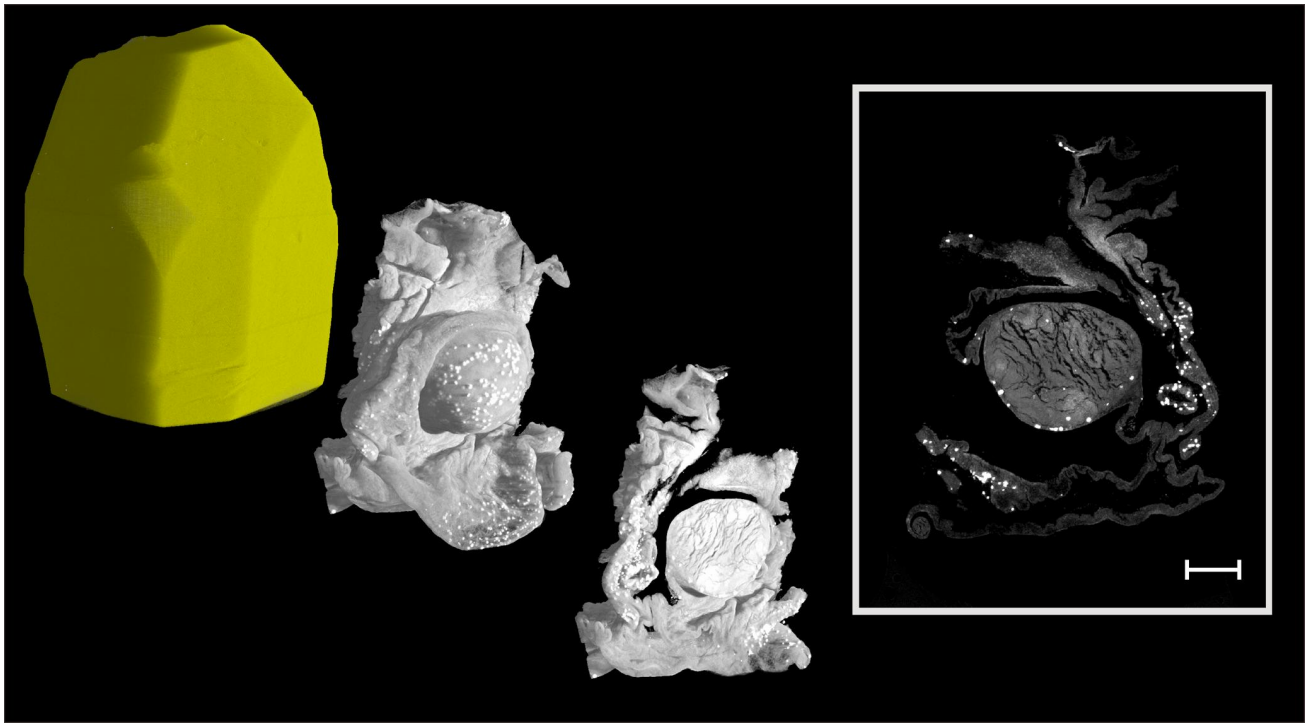

Fig. 2. The 3D representation and the virtual cut of the tomography data of Histoid B demonstrate the complex internal structure. The bar corresponds to 1 mm.

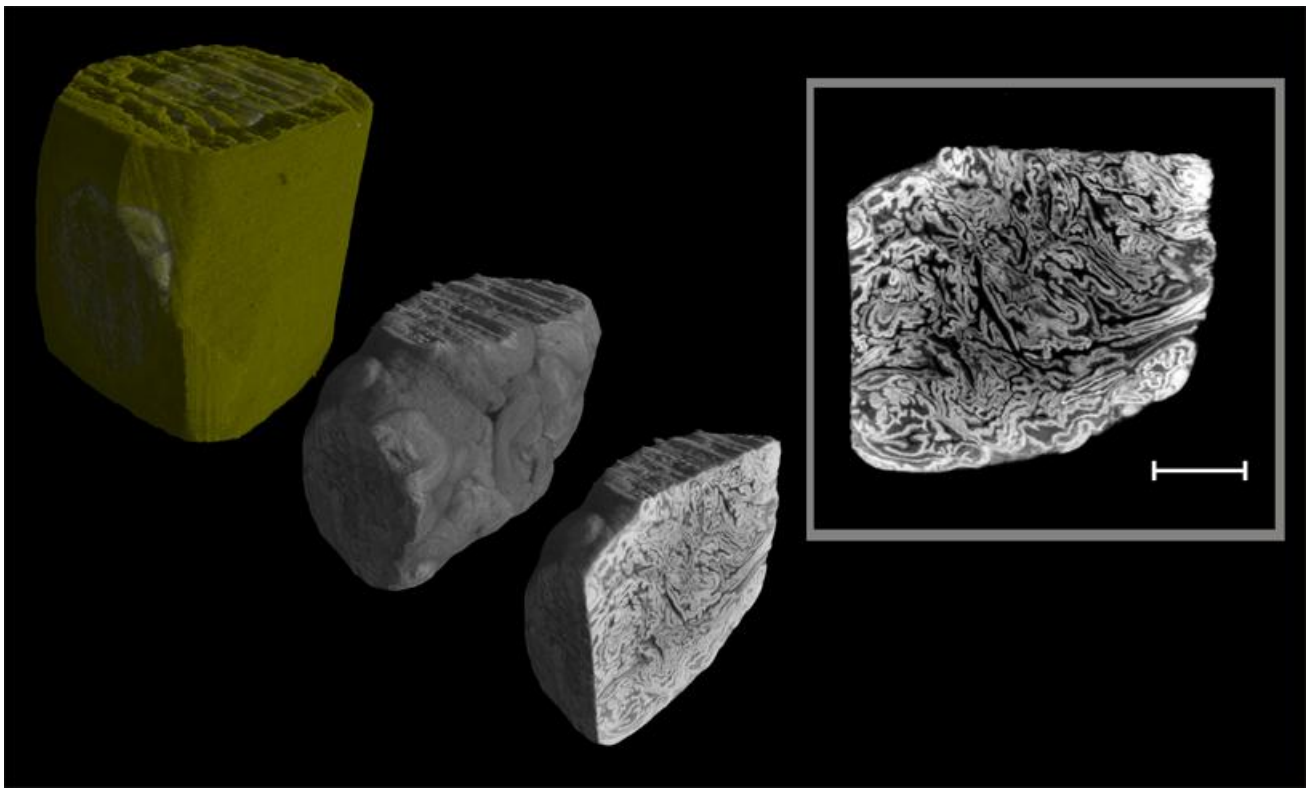

Fig. 3. The tomogram of the Histoid C uncovers membrane folding with channel-like microstructures and a high degree of mineralization that is slightly reduced in the histoid's center. The bar corresponds to 1 mm.

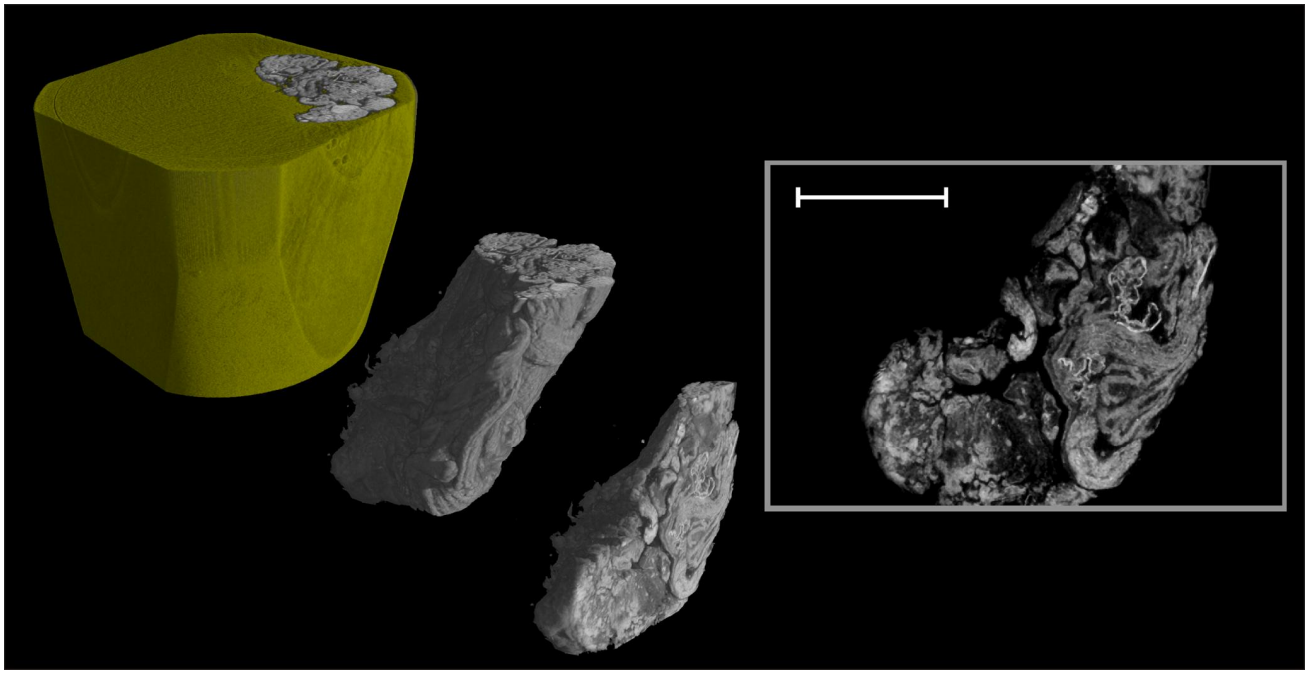

Fig. 4. The Histoid D was cut into two halves prior to embedding. It shows a rather inhomogeneous distribution of cellular features. In the middle of the virtual cut (inset), one clearly recognizes fungal hyphae. The bar corresponds to 1 mm.

The local variation of x-ray absorption indicates regions of different cell densities. The core of the Histoid B shows microstructures of branches and channels quite similar to vascular structures *in vivo*. Consequently, one can assume that this complex 3D system played a crucial role to supply the cells in the inner parts of the histoid with a sufficiently high amount of nutrients and to remove waste from the core. Hence, this microstructure is expected to contribute to the histoid growth during the culturing weeks.

Unfortunately, the density and spatial resolution of the tomogram does not allow identifying isolated cells. The main reason behind is the nature of OsO_4 staining that enhances the absorption of the cell membranes.

Contrary to the other histoids, Histoid C was also grown in mineralizing osteogenic medium (see Table 1). This resulted in progressed mineralization that was physically detected. The histoid appeared relatively stiff, when manually compressed by forceps. Therefore, MMA has been chosen to allow for the histological sectioning of mineralized tissue and to eliminate the need of demineralization as necessary in the case of paraffin embedding. The SRμCT data show a high absorption level. The Histoid C was subjected to osmium ammine-B staining and subsequently embedded into MMA. Osmium ammine-B binds with high affinity to nucleic acids and therefore has been used as a DNA/RNA specific stain.[4, 15] According to the applied staining protocol most of the osmium should be concentrated in the cells nuclei. Hence, there is a higher probability to identify isolated cells. Unfortunately, such features could not be found. This corresponds to the previous finding,[4] where regions with increased osmium were identified but no isolated cells were encountered. As both elements calcium and osmium result in a high degree of X-ray absorption, it is impossible to discriminate between the mineralized matrix and the stained cell nuclei. Based on the *in vitro* observed pronounced stiffness at manual compression testing, one may conclude that the high absorption in the radiographs is mainly due to calcium deposition. The internal microstructure appears as densely packed membranous conglomerate with ECM in-between. The core zone seems to be less mineralized, which can be understood as the result of reduced nutrient supply.

The complex channel-like microstructure might again permit the transportation of nutrients, oxygen and waste. The width distribution of the lower absorbing channels resembles the *in vivo* situation of vascular systems.

Histoid D, which had originally an oblong ovoid shape, was cut into two halves prior to embedding. One halve has been spared for molecular biology investigation. In order to make visible isolated cell structures, Histoid D was again stained with the contrast agent osmium ammine-B but embedded into paraffin. The tomography images reveal also a complex internal microstructure comprising membranous and nodular components interconnected by ECM. This histoid is less

homogeneous and contains highly absorbing cellular structures. The elongated cellular structures form linear chains, which are not straight. They could be identified as the hyphae of the fungus that had infected this long-term 3D cell culture.

To perform the histological examination Histoid A was embedded into paraffin after SRμCT. The slices 4 μm thin were subjected to a series histochemical and immunohistochemical staining. In general, these sections demonstrated a complex internal structure comprising nodular and membranous components. A membrane-like structure overlying the surface histoid and interconnecting the underlying "tissue" is clearly visible as elucidated in Fig. 5. The applied (immuno-)histochemical methods yielded valuable information especially about the chemical composition of the histoid's ECM.

HE staining is a conventional staining method in histopathology. The basic dye hematoxylin gives a blue-purple hue to basophilic structures, whereas the acidic eosin colors eosinophilic structures bright pink. Nucleic acids are basophilic structures, therefore cellular structures like nucleus, ribosomes and cytoplasmic regions rich in RNA appear a blush or purple. The cytoplasm and the proteins of the ECM are rich in eosinophilic components, such as collagen and appear therefore pink. Hydrophobic structures such as adipocytes do not stain very well and to remain clear. HE sections of Histoid A (Fig. 5A) show the presence of abundant ECM rich in collagen. The viable cells are clearly recognized by the slightly darker pink stained cytoplasm and the purple nucleus contained within an intact cellular membrane.

The applied MGT protocol stains the cell nuclei brown-black, cytoplasm red, cartilage and osteoid green. Osteoid is the name given to the organic portion of the bone ECM. It is secreted by the osteoblasts as they begin the process of forming new bone tissue. In other words, osteoid is the pre-state of bone. As the deposited osteoid mineralizes, it and the entrapped/surrouding cells have developed the new bone. Osteoid is composed of a number of specific proteins, whereas col I predominates. Compared to HE, the MGT stained histological sections of Histoid A (Fig. 5B) demonstrated more distinctly the distribution of the abundant non-mineralized ECM, colored in light green. The presence of spots with different degrees of green color saturation is suggestive of some local variations in the ECM composition, which probably result from the different tissue differention stages. The superior contrast of the MGT staining allows to easily distingiush the cell-rich regions that are colored in brown hue.

Antigenic structures like proteins can be specifically detected with immunohistochemical methods, which is impossible with HE or MGT staining. For this reason we performed some immunohistochemical stainings, namely for col I and col IV. With the chromogenic substrate applied in the protocol the detected collagens appear in a red-brown hue.

First we searched for collagen type I, one of the main synthetic products of osteoblasts and the major organic component of the bone ECM [16]. The results show abundant expression of col I, (Fig. 5C) consistent with an osteoid-like histoarchitecture. Here again different degrees of color saturation are seen. For example the membranous structures that are predominantly peripherally located appear darker, suggesting of a high local concentration of this protein. On the other hand the rather acellular nodular regions are paler, which is the result of lower col I concentration on behalf of other ECM constituents, such as proteoglycans or different types of collagens.

As the next step we studied sections of Histoid A for expression of collagen type IV. This protein is found in all basement membranes and characterized by the ability to form complex, covalently linked structural scaffolds, proposed to be required for the basement membrane assembly process.[17] Basement membranes are sheet-like structure of the ECM that are formed at the interfaces between parenchymal cells and their surrounding connective tissues. Basement membranes act as selectively permeable filters or as highly specialized substrates for cellular differentiation and gene expression.[18] With the help of the immunohistochemical staining col IV was detected in the examined slices of Histoid A (Fig. 5D). Compared to col I, the amount is rather low, consistent with the origin of the histoid, as col IV is not a major constituent of the bone ECM. In fact, the presence of col IV can be seen as the indicator of the development of basement membrane-like structures, demonstrating an active histotypic/organotypic organization process within the histoid.

Most of the cells appear eosinophilic with dark blue stained nuclei. The shape and size is concise with mesenchymal cells. In general, the periphery is occupied by denser clusters of cells with rather large nuclei and strong eosinophilic cytoplasm, suggestive of a pre-/osteoblastic phenotype. Cells with smaller nuclei and narrower cytoplasmic space are located mostly in the nodular parts in conjunction with regions with lower col I concentrations. These are likely to be at a more progressed osteoblastic differentiation stage, or may be even pre-osteocytes.

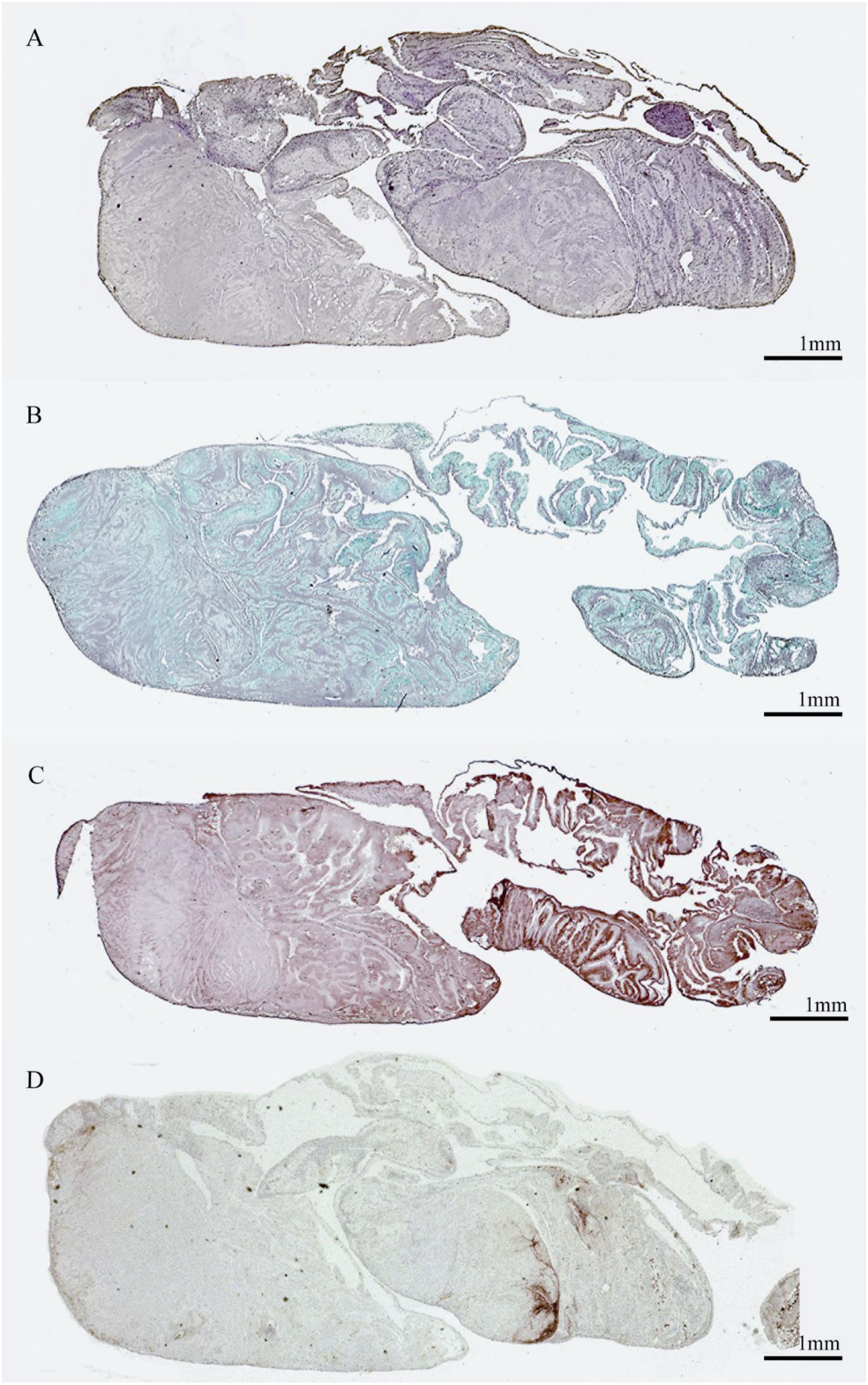

Fig. 5. Histological sections of Histoid A, showing histochemical staining with (A) hematoxylin-eosin and (B) Masson Goldner Trichrome technique, and (C) immunohistochemical staining for collagen type I and (D) collagen type IV.

Adipocytes are clearly distinguished in all histological sections by the spherically shaped microstructures, left after the staining procedures, as fat dissolves easily in alcohol. Yet, some of these cells that have managed to keep the integrity of their cytoplasmic membrane and can be identified especially well on the HE slices as unstained white spots. (Pre-)steoblasts, (pre-)chondroblasts, and (pre-)adipocytes, which usually coexist in the bone marrow spaces, belong to the same cell lineage. The osteo-chondro-adipogenic bone marrow precursor cell has the potential to produce clonal populations with any of these phenotypes or a combination of these.[19] Hence the coexistence of adipocytes with osteoblast-like cells in the histoid is an additional feature demonstrating the complexity of the histoarchitecture.

Staining with the contrast agent OsO_4 resulted in a prominent brown-black coloring of the histoid, because the substance reacts strongly with the lipids of the cell membranes, just like with any other lipid. The histochemical/immunohistochemical results using these kinds of staining have not reached the satisfactory level yet. Currently, suitable protocols for removing the cell bound osmium are under development.

The MMA embedding delivered fragile specimens. Hence, it was impossible to obtain the desired thin sections for histology. Already during the cutting procedure, the sections disintegrated either partially or completely. This behavior is associated with the dense, strongly mineralized superficial layer of the histoid impeded the penetration of the MMA into deeper parts. The resulted hollow spaces forms the fragile structure making histological sectioning impossible.

4. SUMMARY AND CONCLUSION

The SRμCT examination has revealed complex internal micro-morphology of the histoids, principally combining membranous and nodular components in various configurations. Although the histoids exhibited similar spheroid/ovoid outer shape, distinctly different individual histoarchitectural arrangements could be made visible. Variations in the 3D spatial organization of the different histoids, presumably due to their different origin (i.e. donors) and/or cultivation schemes could be clearly recognized. The (immuno-)histochemical studies delivered differentiated information about the cell type, size, functionality and spatial distribution. Some additional details on the chemical composition of the ECM could be extracted.

SRμCT yields detailed, quantitative information about the 3D spatial organization of the histoids. The study of the millimeter-sized, scaffold-free histoids demonstrates that the micro-architecture and the features on the cellular level can be quantified, combining the tomography data with sophisticated computer vision tools. Information about the ECM-composition, cell morphology and type as well as cellular processes such as viability, proliferation and death, however, have still to be provided by the histological methods. The SRμCT together with the advanced visualization techniques is a non-destructive approach suitable for the identification and selection of areas of interest prior to histological sectioning.

This study demonstrates that some embedding and contrasting methods are incompatible with (immuno-)histochemical staining techniques. There is a need for further optimisation of the contrasting-embedding-staining protocols. Because the combination of sufficiently high SRμCT image contrast with minimum distortion of the sections and high quality (immuno-) histochemical staining is the prerequisite for the successful registration/correlation of the data.

ACKNOWLEDGEMENTS

We gratefully acknowledge financial support from the Bayerische Forschungsstiftung. The supply for beamtime at HASYLAB, DESY, Hamburg, Germany is also acknowledged. The authors thank the team at the Institute of Pathology at the University Hospital Basel, especially Thomas Schürch for helping by the preparation of the photos. Special thanks to Saltuk Saldamli, Ph.D. and Stefan Stübinger, DDS for providing technical support during the preparation of the manuscript.

REFERENCES

[1] Harrison, R. G., "Observations on the living developing nerve fiber," Proc Soc Exp Biol Med 4, 140-143 (1907).
[2] Freshney, R. A., [Culture of animal cells: a manual of basic techniques] Wiley-Liss, New York, 1-8 (1994).

[3] Fierz, F. C., Beckmann, F., Huser, M., Irsen, S. H., Leukers, B., Witte, F., Degistirici, Ö., Andronache, A., Thie, M. and Müller, B., "The morphology of anisotropic 3D-printed hydroxyapatite scaffolds," Biomaterials 29, 3799-3806 (2008).
[4] Müller, B., Riedel, M. and Thurner, P. J., "Three-dimensional characterization of cell clusters using synchrotron-radiation-based micro-computed tomography," Microsc Microanal 12, 97-105 (2006).
[5] Thurner, P., Beckmann, F. and Müller, B., "An optimization procedure for spatial and density resolution in hard X-ray micro-computed tomography " Nucl Instr Meth Phys Res B 225, 599-603 (2004).
[6] Thurner, P., Müller, B., Beckmann, F., Weitkamp, T., Rau, C., Müller, R., Hubbell, J. A. and Sennhauser, U., "Tomography studies of human foreskin fibroblasts on polymer yarns " Nucl Instr Meth Phys Res B 200, 397-405 (2003).
[7] Thurner, P., Wyss, P., Voide, R., Stauber, M., Müller, B., Stampanoni, M., Hubbell, J. A., Müller, R. and Sennhauser, U., "Functional micro-imaging of soft and hard tissue using synchrotron light " Proc SPIE 5535, 112-128 (2004).
[8] Thorwarth, G., Saldamli, B., Schwarz, F., Jürgens, P., Leiggener, C., Sader, R., Haeberlein, M., Assmann, W. and Stritzker, B., "Biocompatibility of doped diamond-like carbon coatings for medical implants," Plasma Proc Polym 4(SI), S364-S368 (2007).
[9] Levin-Zaidman, S., Frenkel-Krispin, D., Shimoni, E., Sabanay, L., Wolf, S. G. and Minsky, A., "Ordered intracellular reca-DNA assemblies: A potential site of in vivo reca-mediated activities," Proc Natl Acad Sci USA 97, 6791-6796 (2000).
[10] Beckmann, F., Donath, T., Dose, T., Lippmann, T., Martins, R. V., Metge, J. and Schreyer, A., "Microtomography using synchrotron radiation at DESY: current status and future developments " Proc SPIE 5535, 1-10 (2004).
[11] Müller, B., Thurner, P., Beckmann, F., Weitkamp, T., Rau, C., Bernhardt, R., Karamuk, E., Eckert, L., Buchloh, S., Wintermantel, E., Scharnweber, D. and Worch, H., "Three-dimensional evaluation of biocompatible materials by microtomography using synchrotron radiation," Proc SPIE 4503, 178-188 (2002).
[12] Kak, A. C. and Slaney, M., [Principles of Computerized Tomographic Imaging], SIAM Classics in Applied Mathematics vol. 33), Philadelphia, (2001).
[13] Müller, B., Bernhardt, R., Weitkamp, T., Beckmann, F., Bräuer, R., Schurigt, U., Schrott-Fischer, A., Glueckert, R., Ney, M., Beleites, T., Jolly, C. and Scharnweber, D., "Morphology of bony tissues and implants uncovered by high-resolution tomographic imaging " Int J Mater Res 98 (7), 613-621 (2007).
[14] Romeis, B., [Mikroskopische Technik/ Romeis], Urban und Schwarzenderg, München, 235 and 500 (1989).
[15] Vazquez-Nin, G. H., Biggiogera, M. and Echeverria, O. M., "Activation of osmium ammine by SO2-generating chemicals for EM Feulgen-type staining of DNA," Eur J Histochem 39, 101-106 (1995).
[16] Kern, B., Shen, J., Starbuck, M. and Karsenty, G., "Cbfa1 Contributes to the Osteoblast-specific Expression of type I collagen Genes," J Biol Chem 276(10), 7101-7107 (2001).
[17] Kühn, K., "Basement membrane (type IV) collagen," Matrix Biol 14, 439-445 (1994).
[18] Pöschl, E., Schlotzer-Schrehardt, U., Brachvogel, B., Saito, K., Ninomiya, Y. and Mayer, U., "Collagen IV is essential for basement membrane stability but dispensable for initiation of its assembly during early development," Development 131 (7), 1619-1628 (2004).
[19] Young, H. E., Duplaa, C., Katz, R., Thompson, T., Hawkins, K. C., Boev, A., Heaton, M., Sood, R., Ashley, D., Stout, C., Morgan, J. H. I., Uchakin, P. N., Rimando, M., Long, G. F., Thomas, C., Yoon, J.-I., Park, J. E., Hunt, D. J., Walsh, N. M., Davis, J. C., Lightner, J. E., Hutchings, A. M., Murphy, M. L., Boswell, E., McAbee, J. A., Gray, B. M., Piskurich, J., Blake, L., Collins, J. A., Moreau, C., Hixson, D., Bowyer, F. P. I. and Black, A. C. J., "Adult-derived stem cells and their potential for use in tissue repair and molecular medicine," J Cell Mol Med 9, 753-769 (2005).